WAVE MOTION 11 (1989) 65-76
NORTH-HOLLAND

A STUDY OF WAVE INTERACTIONS WITH FLANGED WAVEGUIDES AND CAVITIES USING THE ON-SURFACE RADIATION CONDITION METHOD

Jeffrey BLASCHAK

Department of Electrical Engineering, The Technological Institute, Northwestern University, Evanston, IL 60208, U.S.A.

Gregory A. KRIEGSMANN

Department of Engineering Sciences and Applied Mathematics, The Technological Institute, Northwestern University, Evanston, IL 60208, U.S.A.

Allen TAFLOVE

Department of Electrical Engineering, The Technological Institute, Northwestern University, Evanston, IL 60208, U.S.A.

Received 29 January 1988

The scattering of a plane wave from the open end of a flanged, parallel plate waveguide is approximately solved using the On-Surface Radiation Condition method. Simple explicit formulae are given for the field within the waveguide and for the bistatic cross-section. In addition, our theory also gives an approximate solution to the associated open cavity problem, which is formed when the waveguide is terminated by a short circuit positioned a finite distance from the aperture. These problems serve as prototypes for receiving antennae and open resonators respectively. Numerical results are presented which confirm the accuracy of the OSRC method. An interesting byproduct of our analysis is the approximate prediction of the complex eigenfrequencies of the open resonator.

1. Introduction

In this paper, we study the interaction of waves with an infinitely flanged, parallel-plate waveguide which is either infinite in extent or short-circuited at a finite distance along its length. (See Fig. 1.) The former case serves as a prototype for both receiving antennas and simple re-entrant structures while the second models a basic Helmholtz resonator. We restrict our attention here to scalar waves so that the results obtained are applicable to acoustics and electromagnetics in two dimensions.

The method we develop is approximate and is based upon the On-Surface Radiation Condition method (OSRC) which has been recently developed to analytically model the scattering of waves by convex targets [1, 2, 3]. In this method a differential operator (radiation boundary operator) which annihilates the scattered field as $r \to \infty$ is applied directly on the *surface* of a target. Then, both the field and its normal derivative can be deduced from this approximate condition and the given boundary condition for the scatterer.

In this paper, we apply an annihilating operator to the scattered field in the *aperture* of a parallel-plate waveguide and again obtain a relationship between the field and its normal derivative. Combining this result with the continuity of the total field and its normal derivative in the aperture, we effectively decouple the waveguide region from the half-space $z < 0$. This allows us to explicitly determine the field within the waveguide without recourse to matrix inversion [4], ray tracing [5, 6], or hybrid method [7]. From this result, we also obtain (with the aid of a Green's function representation) the scattered field in the region $z < 0$.

The results of our approximate OSRC theory for penetrating and scattered fields compare extremely well with detailed numerical computa-

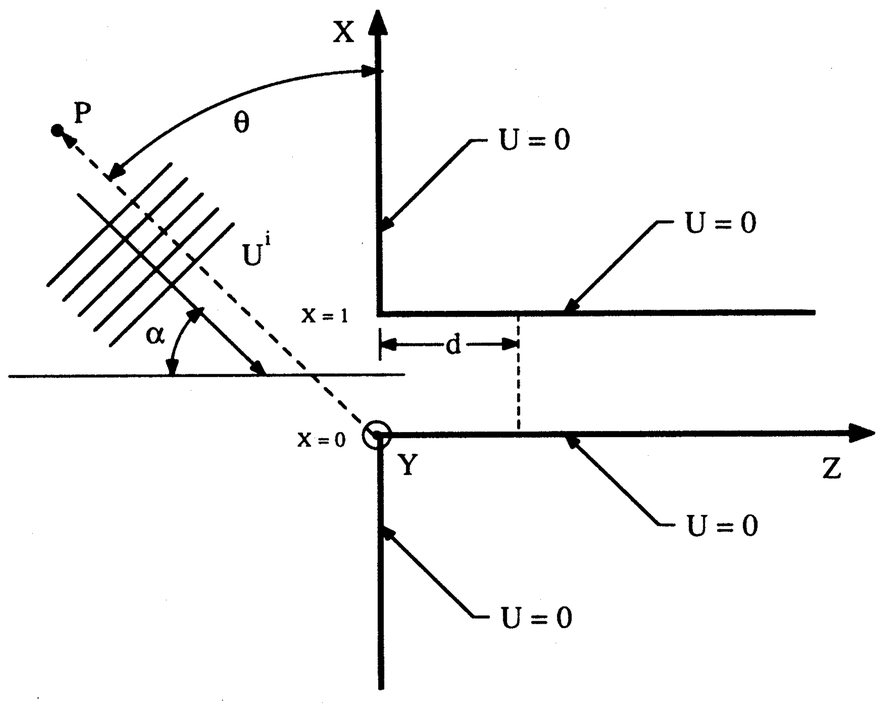

Fig. 1. Plane wave at angle α illuminates the open end of a flanged, infinite, parallel plate waveguide. The cavity problem is created by placing a short at the position $z = d$.

tions obtained using a time-dependent finite difference scheme (FD-TD) [8, 9] applied directly to the field equations. Excellent agreement is found for both the infinite waveguide case and the short-circuited waveguide. In the former case a key OSRC result shows that the scattered field exhibits "resonant" frequency behavior. This is again verified by the FD-TD scheme. Moreover, we are able to use our approximate results to obtain an estimate of the open resonator's "eigenfrequencies". These are complex numbers whose imaginary parts dictate the rate at which energy leaks away from the open cavity.

The remainder of this paper will now be outlined. Section 2 contains the formulation of the scattering problem and Section 3 includes the extension of the OSRC method that is required to handle the present problem. Section 4 contains the results of several illustrative examples which clearly indicate the accuracy of our approximate method. And finally, Section 5 includes a derivation of the approximate "eigenfrequencies" of our prototype Helmholtz resonator.

2. Formulation

The geometry of the flanged parallel-plate waveguide is shown in Fig. 1. Here x and z represent nondimensional variables which have been scaled with respect to the guide's physical width a. The total field, $U(x, z, k)$ satisfies the Helmholtz equation

$$\Delta U + k^2 U = 0; \quad z < 0 \text{ with } |x| < \infty,$$
$$\text{and } z > 0 \text{ with } 0 < x < 1, \tag{2.1a}$$

where $k = \omega a / c$ and c is the wave's speed, and the boundary condition

$$U = 0, \qquad (x, z) \in R \tag{2.1b}$$

where R represents the boundary composed of the flange and the waveguide's walls. A time dependence of $\exp(i\omega t)$ has been assumed and will be suppressed in the subsequent equations.

An incident plane wave given by

$$U_{\text{inc}}(x, z, k) = \exp[-ik(z \cos \alpha - x \sin \alpha)] \tag{2.2}$$

impinges upon this target and scatters from it. Accordingly, the total field U^- in the region $z < 0$ is given by

$$U^- = U_{\text{inc}}(x, z, k) - U_{\text{inc}}(x, -z, k) + u(x, z, k); \quad z < 0, \tag{2.3}$$

where the second term in (2.3) is the wave reflected by the flange and u is the scattered field caused by the waveguide. The latter satisfies the Helmholtz equation (2.1a) for $z < 0$ and the Sommerfeld radiation condition

$$\lim_{r \to \infty} \sqrt{r} \left[\frac{\partial}{\partial r} + iku \right] = 0 \tag{2.4}$$

where $r = [x^2 + z^2]^{1/2}$.

When the wall at $z = d$ (the short circuit) is not present, the total field in the waveguide, U^+, is given by

$$U^+ = \sum T_n \exp(-ik_n z) \times \sin(n\pi x); \quad z > 0. \tag{2.5a}$$

When the wall at $z = d$ is present, the total field in the waveguide is given by

$$U^+ = \sum T_n \{\exp(-ik_n z) - \gamma_n \exp(ik_n z)\} \times \sin(n\pi x); \quad 0 < z < d. \tag{2.5b}$$

The summation in (2.5) runs over all positive integers n. The propagation constants k_n and the reflection coefficients γ_n are defined respectively by

$$k_n = [k^2 - (n\pi)^2]^{1/2}, \tag{2.6a}$$

$$\gamma_n = \exp(-2ik_n d). \tag{2.6b}$$

The transmission coefficients T_n are to be determined.

To complete the formulation of our boundary value problem, we demand that U and $\partial/\partial z\, U$ be continuous along the waveguide aperture $z = 0$ and $0 < x < 1$, that is,

$$U^-(x, 0, k) = U^+(x, 0, k), \qquad 0 < x < 1, \tag{2.7a}$$

$$\frac{\partial}{\partial z} U^-(x, 0, k) = \frac{\partial}{\partial z} U^+(x, 0, k), \quad 0 < x < 1. \tag{2.7b}$$

Finally, using standard Green's function arguments, we find that the scattered field is given in terms of $U(x, 0, k)$ by

$$u(x, z, k) = \int_0^1 U(x', 0, k)\, \dot{H}_0^{(1)}(kR)\, \frac{dx'}{R} \tag{2.8a}$$

where $\dot{H}_0^{(1)}$ is the derivative of the zeroeth order Hankel function and R is defined by

$$R = [(x - x')^2 + z^2]^{1/2}. \tag{2.8b}$$

Here we note that $U(x, 0, k) = u(x, 0, k)$ by (2.3).

We can physically interpret the above scattering problem in terms of electromagnetics or acoustics. In the electromagnetic case, U would be the amplitude of the electric field vector which is polarized along the y-axis, and the waveguide and flange would be perfectly conducting. In the acoustics case, U would be proportional to the pressure, and the waveguide and flange would be acoustically "soft".

3. Extension of the OSRC method

The scattered field u satisfies the radiation boundary condition [10, 11]

$$\frac{\partial}{\partial r} u + [\frac{2}{r} + ik]u - \frac{Lu}{2r^2(ik + 1/r)} = O(r^{-5}) \tag{3.1a}$$

as $r \to \infty$ where L is defined by

$$Lu = \left[\frac{\partial^2}{\partial \theta^2} u + \frac{u}{4}\right]. \tag{3.1b}$$

In our previous work [1] we applied (3.1) directly on the surface of a two-dimensional convex target by setting the $O(r^{-5})$ term equal to zero and replacing r^{-1} by κ, $r^{-2}\partial^2 u/\partial\theta^2$ by $\partial^2 u/\partial s^2$, and $\partial u/\partial r$ by $\partial u/\partial \nu$. Here, κ is the curvature of the target's boundary curve, s is the arclength, and $\partial/\partial\nu$ is the outgoing normal derivative.

We now apply the same operator to the scattered field u in the aperture of the flanged waveguide. We set κ equal to zero because the aperture is planar, replace s by x in the second tangential derivative, and ν by $-z$ in the normal derivative. This yields the approximate condition

$$Bu = \frac{\partial}{\partial z} u - iku - \frac{i}{2k} \frac{\partial^2}{\partial x^2} u = 0,$$
$$0 < x < 1,\ z = 0. \tag{3.2}$$

We note here that the operator B can also be obtained by an approximate factoring of the Helmholtz equation in rectangular coordinates [12].

Next, we deduce from (2.7) and the definition of the operator B that

$$BU^+ = BU^-, \quad 0 < x < 1,\ z = 0. \tag{3.3}$$

Inserting (2.3) into the right-hand side of (3.3) and using (3.2), we find that

$$BU^+ = g(x), \quad 0 < x < 1,\ z = 0 \tag{3.4a}$$

where the function $g(x)$ is defined by

$$g(x) = -2ik \cos\alpha \exp(ikx \sin\alpha),$$
$$0 < x < 1. \tag{3.4b}$$

Applying the operator B to U^+ given by (2.5) and combining this result with (3.4), we obtain

$$\sum G_n T_n \sin(n\pi x) = g(x), \quad 0 < x < 1, \tag{3.5a}$$

$$\sum J_n T_n \sin(n\pi x) = g(x), \quad 0 < x < 1, \tag{3.5b}$$

where the sums are again over integer n and

$$G_n = -\mathrm{i}\left[k_n + k - \frac{1}{2k}(n\pi)^2 \right], \tag{3.6a}$$

$$J_n = -\mathrm{i}\left[k_n(1+\gamma_n) + k(1-\gamma_n) - \frac{1}{2k}(1-\gamma_n)(n\pi)^2 \right]. \tag{3.6b}$$

Finally, we use the Fourier inversion formula to solve (3.5) for the unknown coefficients T_n. We find that

$$T_n = 4\mathrm{i}k \cos\alpha \, g_n(k \sin\alpha)/G_n \tag{3.7a}$$

for the flanged waveguide and

$$T_n = 4\mathrm{i}k \cos\alpha \, g_n(k \sin\alpha)/J_n \tag{3.7b}$$

for the short-circuited waveguide (open resonator), where $g_n(\zeta)$ is

$$g_n(\zeta) = -\begin{cases} \dfrac{n\pi}{(n\pi)^2 - \zeta^2}\left[1 - (-1)^n \exp(\mathrm{i}\zeta)\right], \\ \qquad \zeta \neq n\pi, \\ \dfrac{\mathrm{i}}{2}, \quad \zeta = n\pi. \end{cases} \tag{3.8}$$

The approximate field within the waveguide is obtained by combining (2.5a), (3.6a), (3.7a), and (3.8). The analogous expression for the field within the open resonator is given by (2.5b), (3.6b), (3.7b), and (3.8).

The scattered field is given by (2.7) with $U(x, 0, k)$ replaced by either (2.5a) or (2.5b). By using standard far-field approximations in (2.8) we find that, as $r \to \infty$,

$$u(x, z, k) \sim A(\theta, k) \frac{\mathrm{e}^{-\mathrm{i}kr}}{\sqrt{r}}, \tag{3.9a}$$

$$A(\theta, k) = k \sin\theta (2\pi k)^{-1/2} \times \exp(-\mathrm{i}\pi/4) \sum T_n g_n(\cos\theta) \tag{3.9b}$$

where $g_n(\zeta)$ is defined in (3.8) and θ is measured from the x-axis in a counter-clockwise direction (see Fig. 1).

4. Illustrative examples

The accuracy of (2.5) and our approximations (3.7) is now demonstrated in two illustrative problems. In the first example, a flanged infinite waveguide is illuminated by a plane wave having $k \approx 8$ and impinging at an incident angle α as shown in Fig. 1. Two values of α are chosen: $\alpha = 0°$ (normal incidence) and $\alpha = 30°$. The second example is the associated cavity problem created by terminating the waveguide with a short circuit at a distance d from the aperture. For both examples, we compute the field distribution at $z = \frac{2}{3}$ using (2.5) and the bistatic cross-section of the scattered field, in the region $z < 0$, using (3.9).

The accuracy of the OSRC method is assessed by comparing its results to those obtained using a finite difference scheme applied directly to the time-dependent field equations. The accuracy of finite difference time domain (FD-TD) methods on the problems we consider here is well established [8, 9]. In the first case, the infinite waveguide is modeled using FD-TD by a sufficiently long, finite waveguide which is terminated by a short. In the FD-TD simulation, this structure is illuminated by a sinusoidal incident plane wave and time-stepped for a sufficient number of wave cycles to allow the numerical solution within two wavelengths of the aperture to reach the time-harmonic steady-state. The waveguide length and number of time steps is carefully chosen to guarantee that reflections from the terminated end are not present in the aperture region of interest. For the second example, the depth of the cavity d is selected to be the same as the aperture width. The FD-TD cavity simulation is performed on a domain considerably smaller than that for the infinite waveguide. Here, however, more wave cycles are required to be time-stepped for the simulation to achieve the time-harmonic steady-state

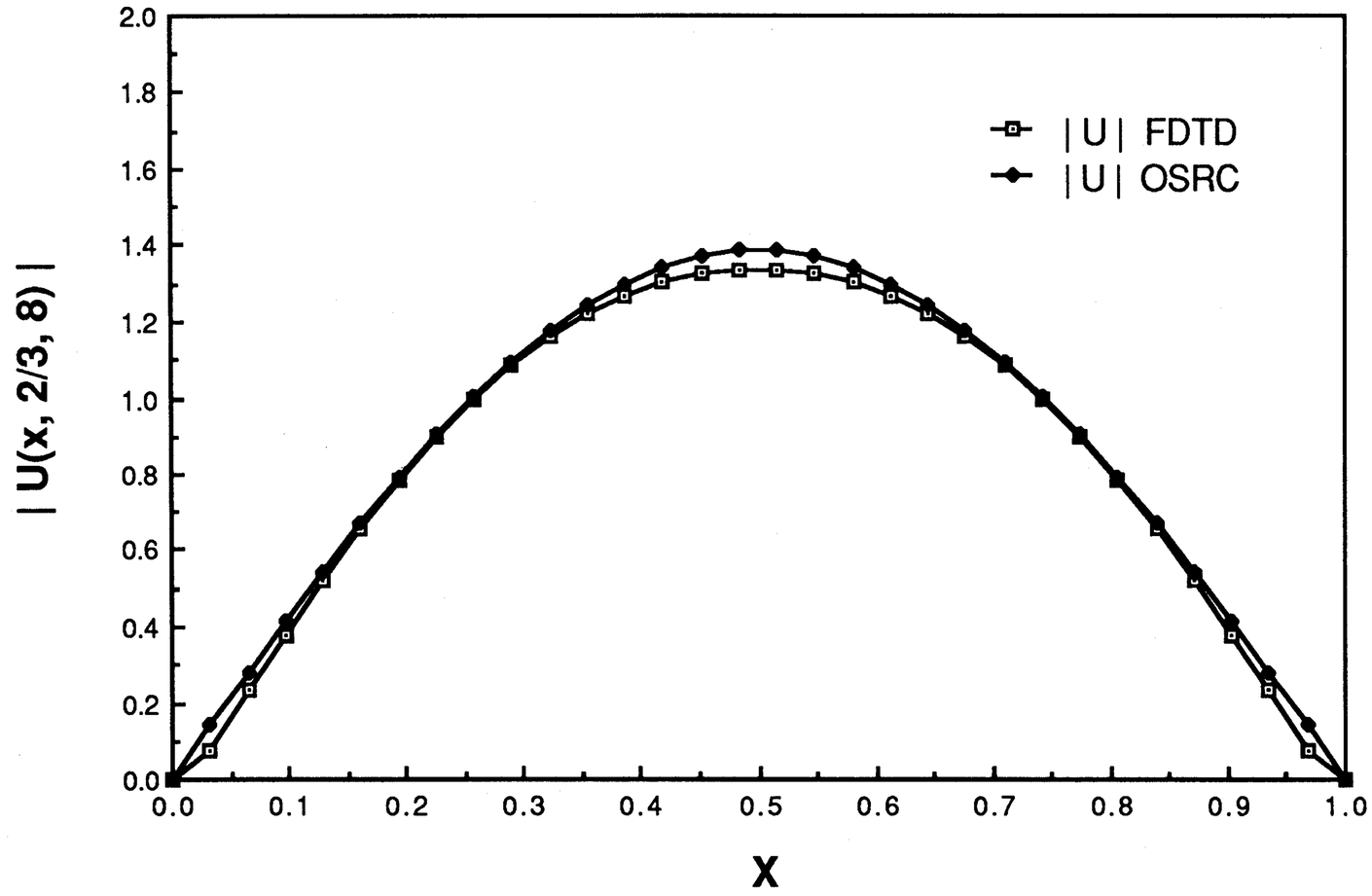

Fig. 2. Distribution of field magnitude inside infinite waveguide at $z=\frac{2}{3}$ for $\alpha=0°$.

due to the structure's ability to trap energy for a period of time.

With $k\approx 8$, the dimensions of the infinite waveguide are such that only the first two modes propagate. The results of our OSRC and FD-TD calculations for the infinite waveguide example are presented in Figs. 2 through 7. Figs. 2 and 3 show respectively the magnitude and phase of $U^{+}(x, 0.666, 8)$ for $\alpha=0°$. For this case, only the first term in the sum (2.5) need be evaluated because $T_2=0$, by symmetry. The corresponding results for $\alpha=30°$ are presented in Figs. 4 and 5

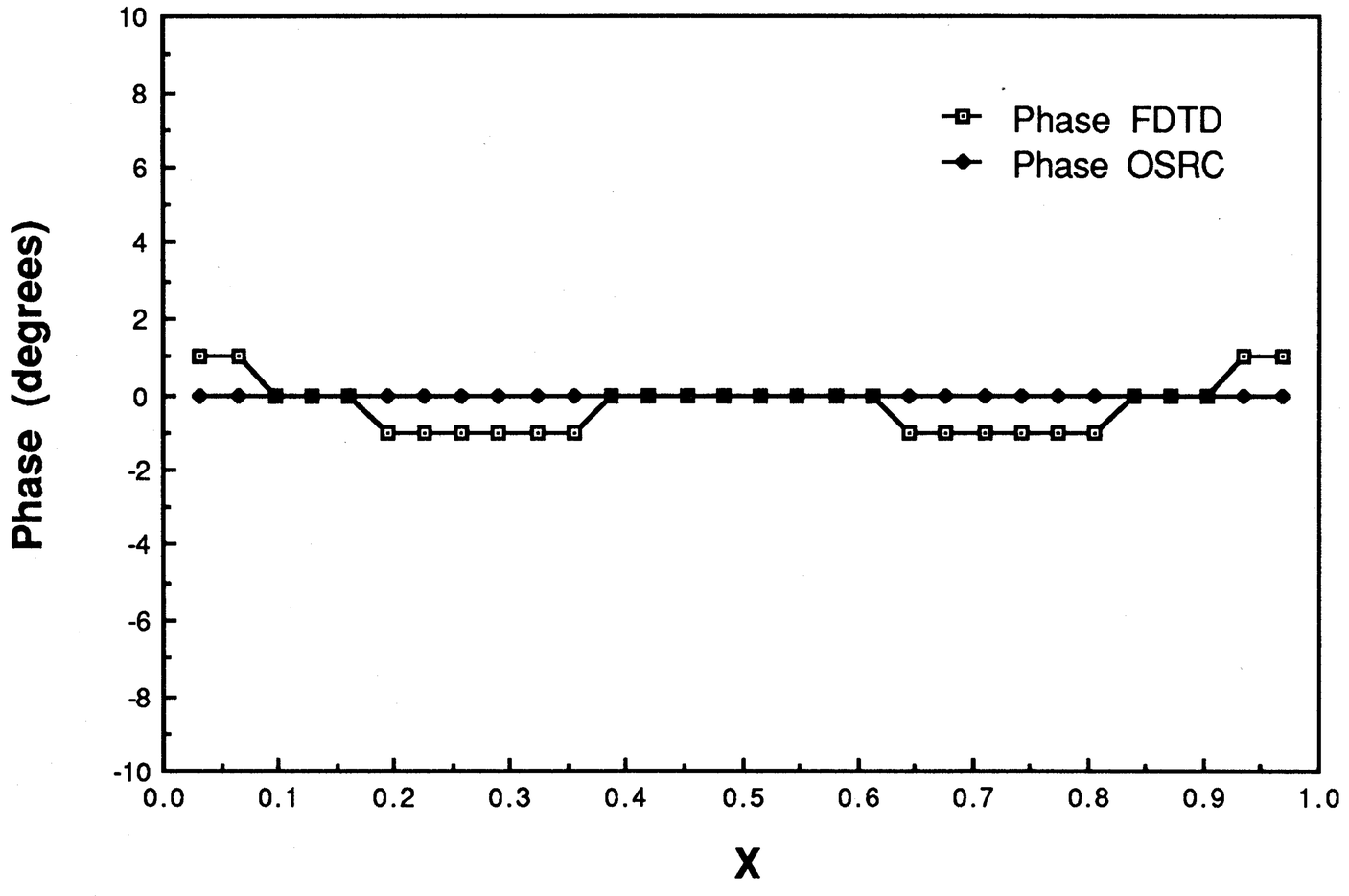

Fig. 3. Distribution of field phase inside infinite waveguide at $z=\frac{2}{3}$ for $\alpha=0°$.

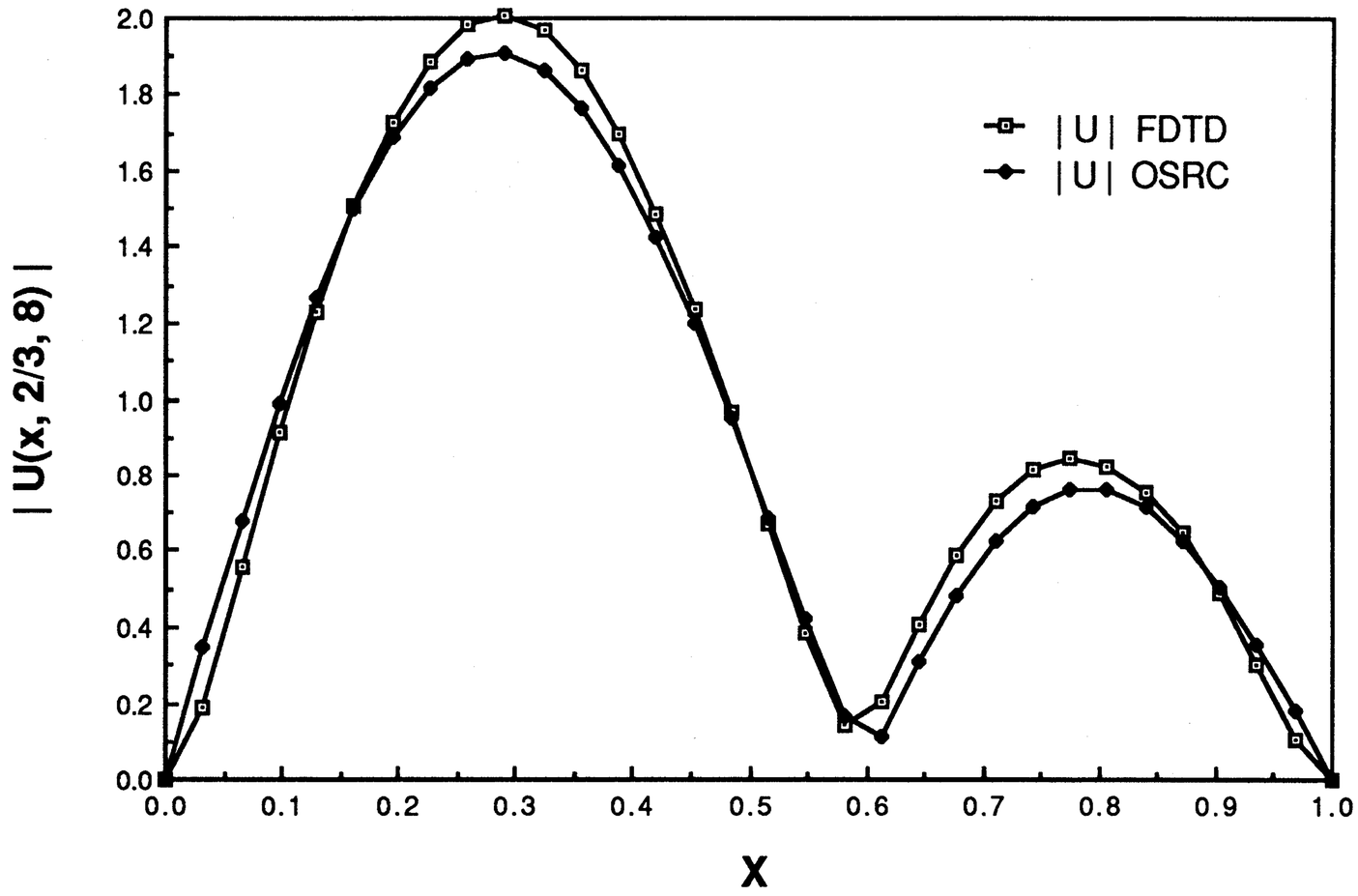

Fig. 4. Same as Fig. 2 except $\alpha = 30°$.

respectively. Both propagating modes are excited for this case and thus, only the first two terms in (2.5) are needed for our approximate solution. These excellent results indicate that the on-surface radiation condition operator effectively couples the energy of the incident plane wave into the propagating waveguide modes. We have also included several evanescent modes in (2.5) and found little change in the far field and a deleterious change in the aperture field.

The bistatic cross section of the scattered field in the region, $z < 0$, is shown in Figs. 6 and 7 for

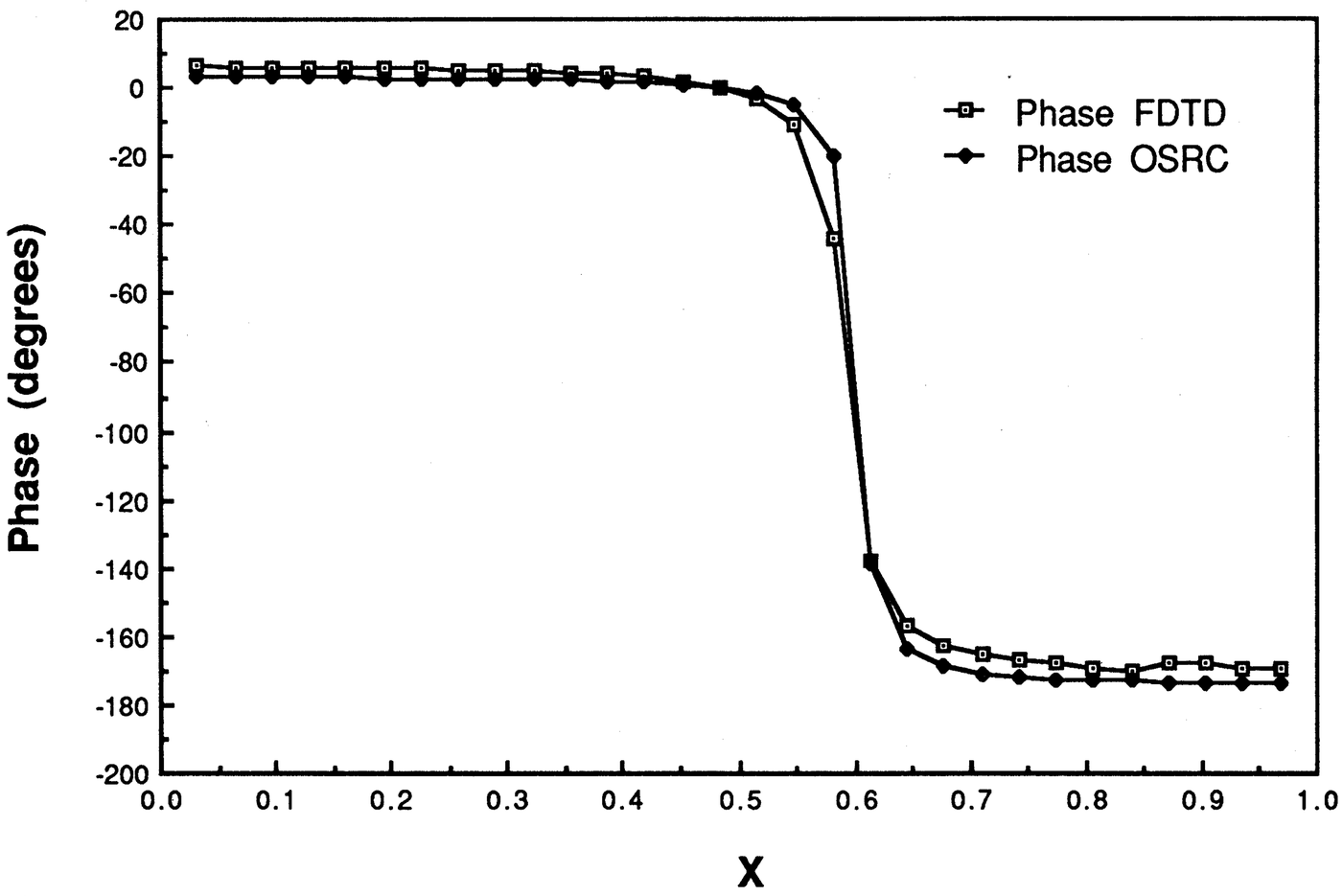

Fig. 5. Same as Fig. 3 except $\alpha = 30°$.

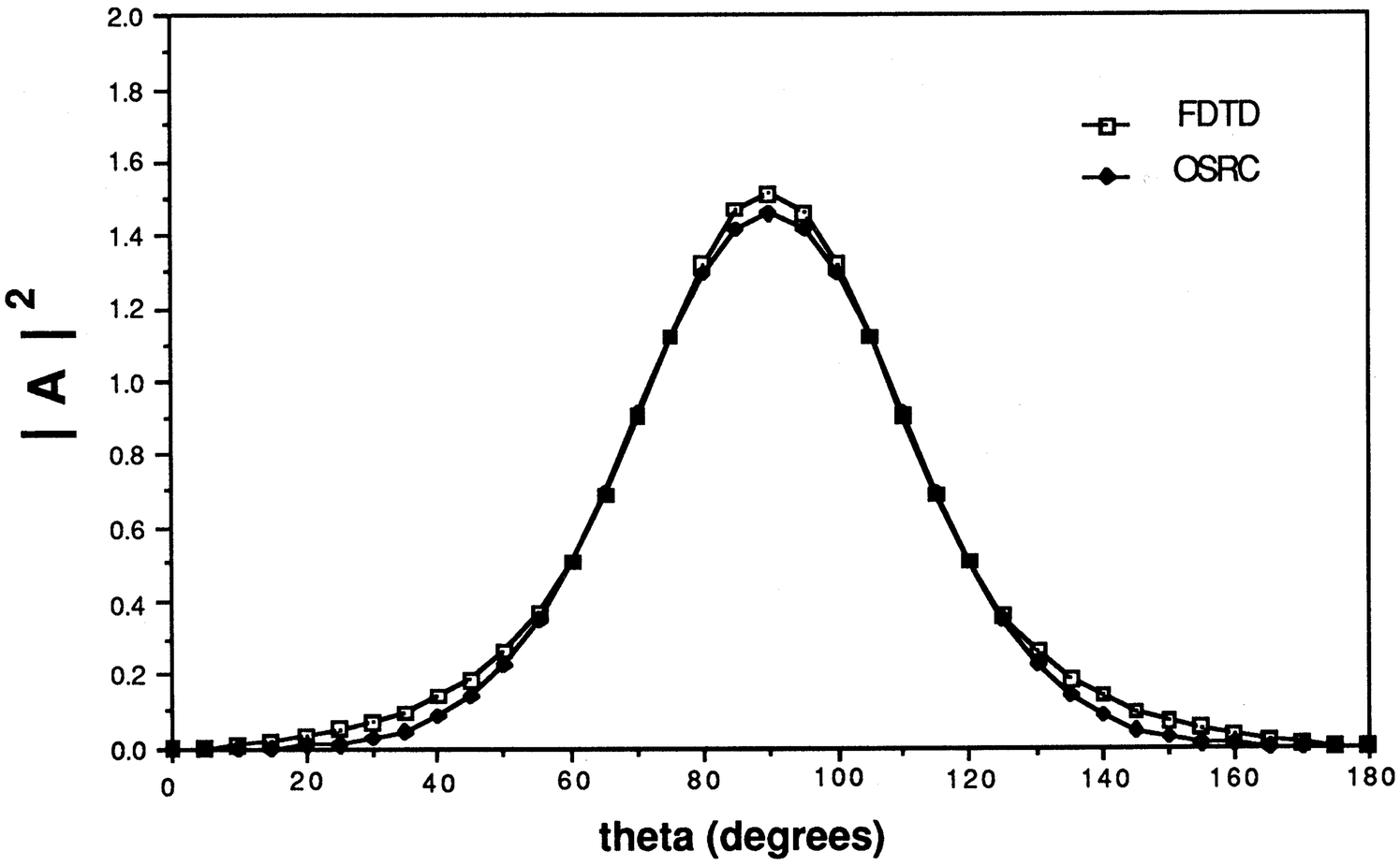

Fig. 6. Bistatic cross-section for the field scattered from the aperture of the infinite waveguide in the region $z<0$ for $\alpha=0°$. The angle θ is as shown in Fig. 1.

each value of α. Again, excellent agreement is observed between the results obtained using the on-surface radiation condition approach and those obtained by the FD-TD simulation. It should be noted that the amount of computer time required to evaluate the formulae generated by the OSRC theory is negligible (less than 0.006%) compared to that of a typical FD-TD simulation for the idealized problems considered here.

The results of the companion calculations for the open resonator example are presented in Figs. 8 through 13. These results are for $k\approx 8$ and

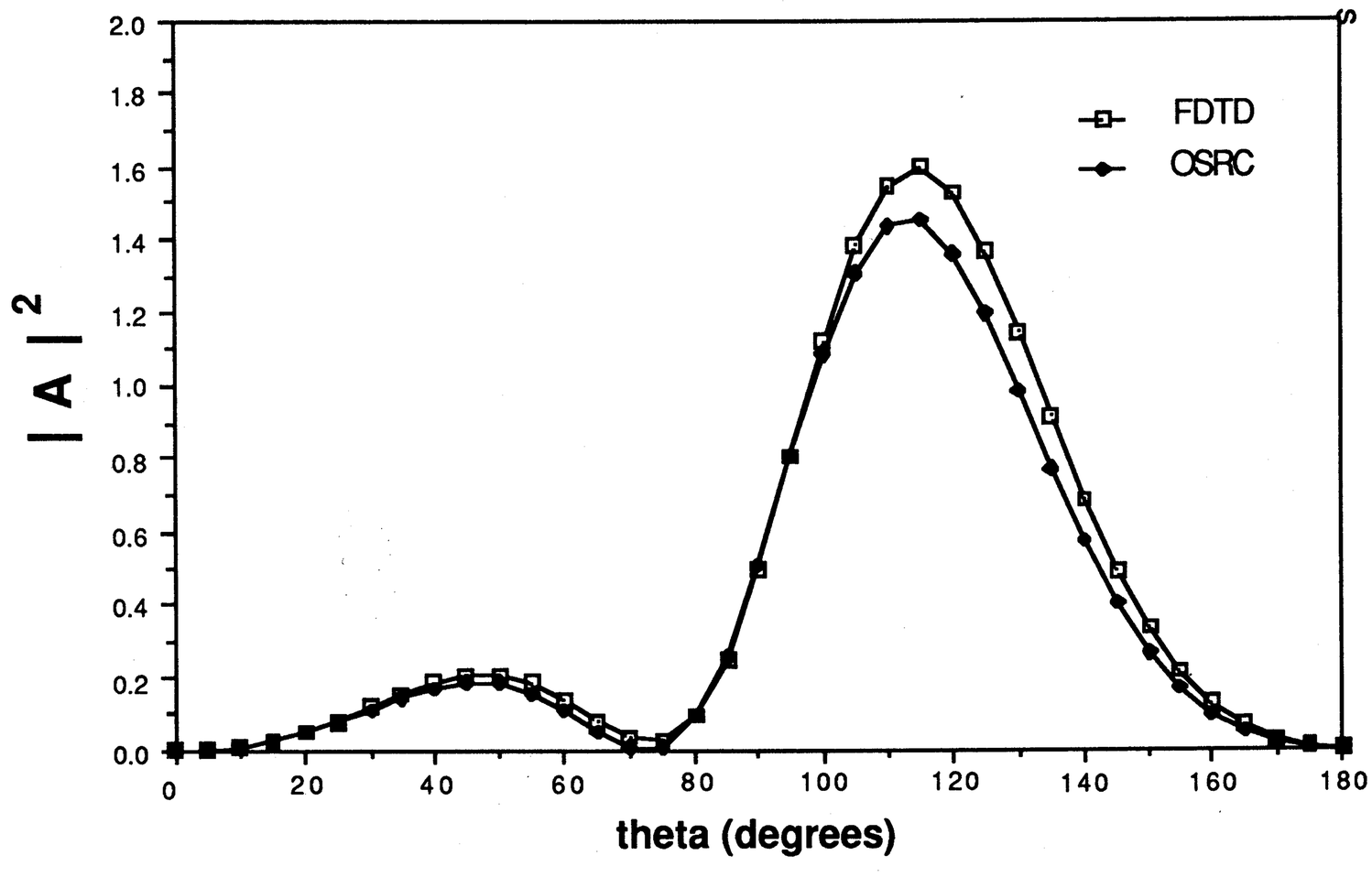

Fig. 7. Same as Fig. 6 except $\alpha=30°$.

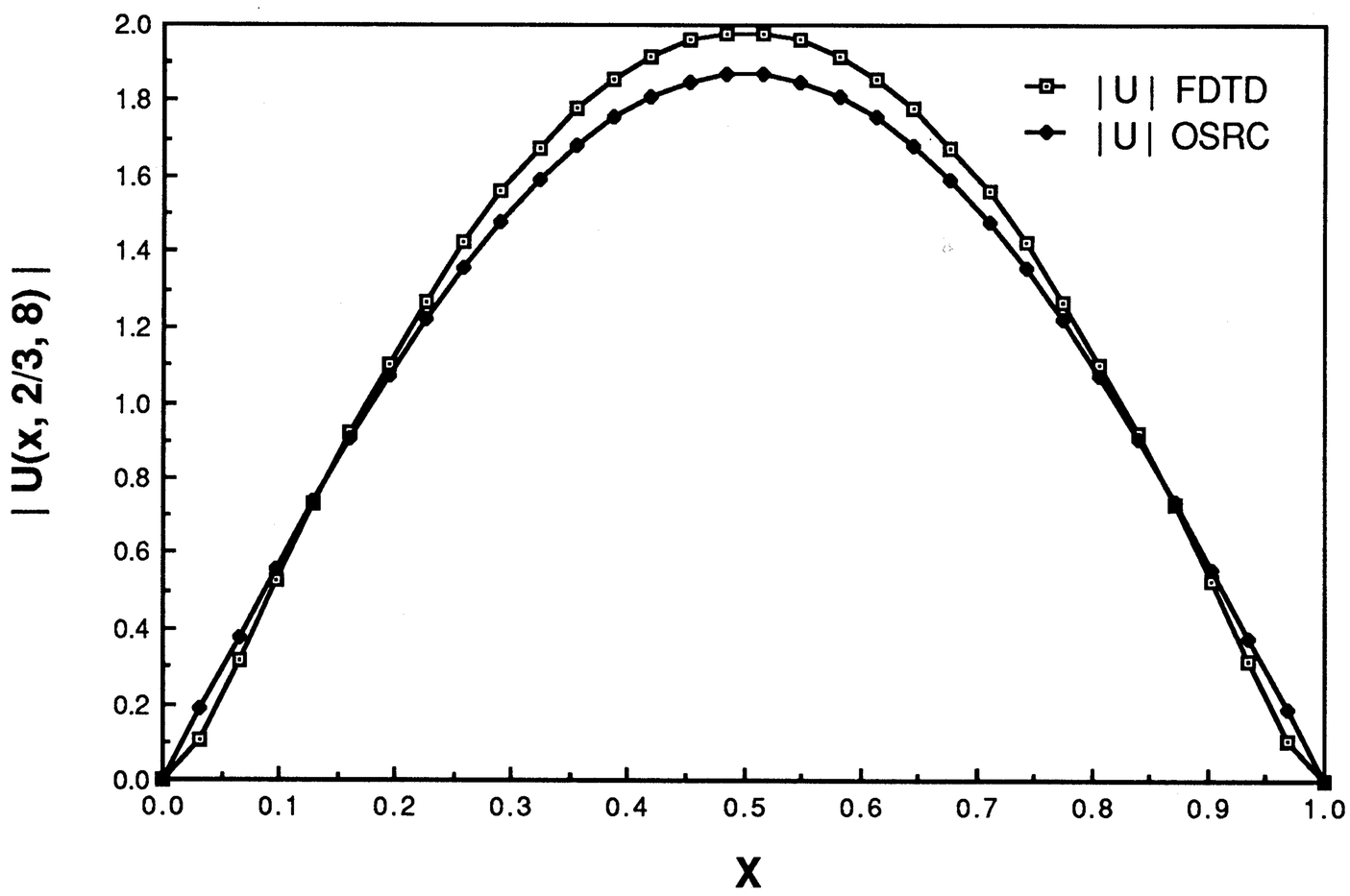

Fig. 8. Distribution of field magnitude inside the cavity at $z=\frac{2}{3}$ for $\alpha=0°$.

$a=d=1$. Once again, good agreement between the OSRC results and the FD-TD simulations is observed.

Figure 14 shows the OSRC and FD-TD computed values for $U^{+}(0.5, 0.0, k)$ as a function of k. The FD-TD result is obtained by simulating an impulsive plane wave followed by an FFT. The agreement is good for $3.5<k<8$ and deteriorates outside this band, which approximates the range of frequency components in the impulsive plane wave. The error at very low frequencies is caused by the OSRC method, which is consistent with our

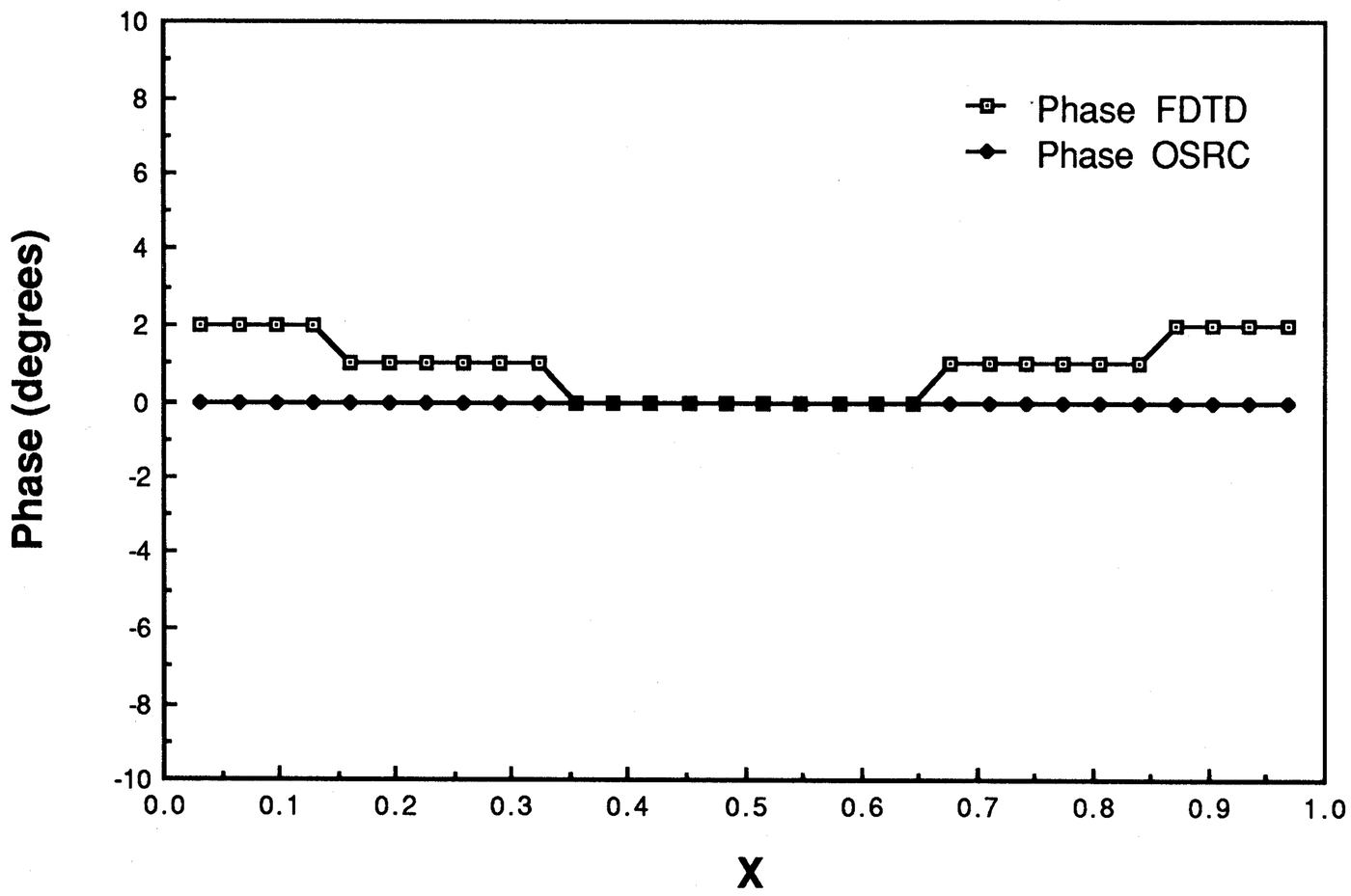

Fig. 9. Distribution of field phase inside the cavity at $z=\frac{2}{3}$ for $\alpha=0°$.

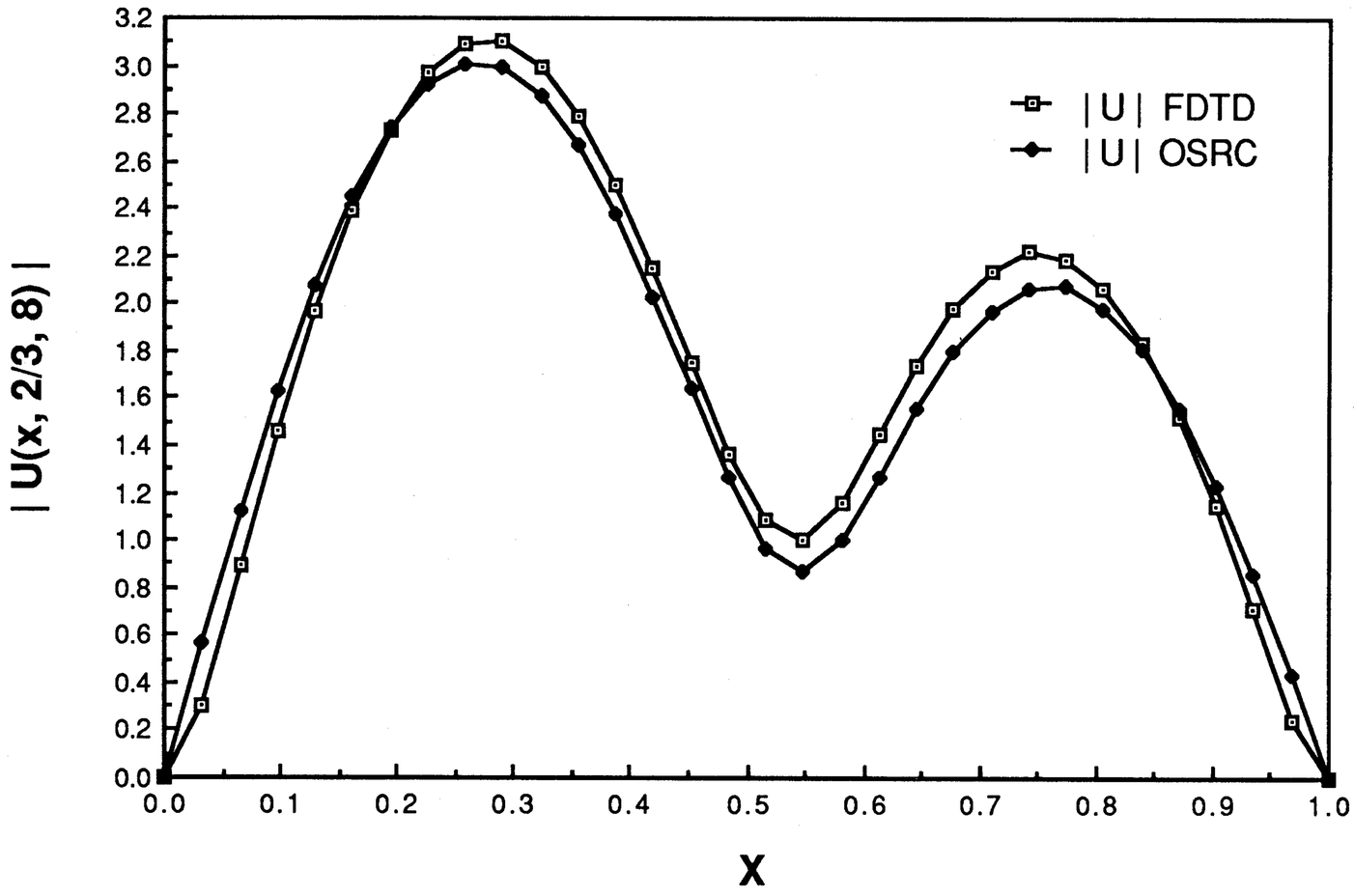

Fig. 10. Same as Fig. 8 except $\alpha = 30°$.

previous observations [1], and the onset of cut-off which occurs at $k = \pi$. Additional errors can occur with the OSRC solution at other cut-off frequencies $k = n\pi$ (if those modes are excited) because the energy is not out-going in the aperture. In the present case, the odd modes are excited while the even ones are not. The peaks (except for the first one) and sharp nulls in the response occur roughly at the eigenfrequencies of the "closed" cavity

$$k^{c}_{n,m} = \pi[n^2 + m^2/d^2]^{1/2} \tag{4.1}$$

and show a resonance behavior for the open struc-

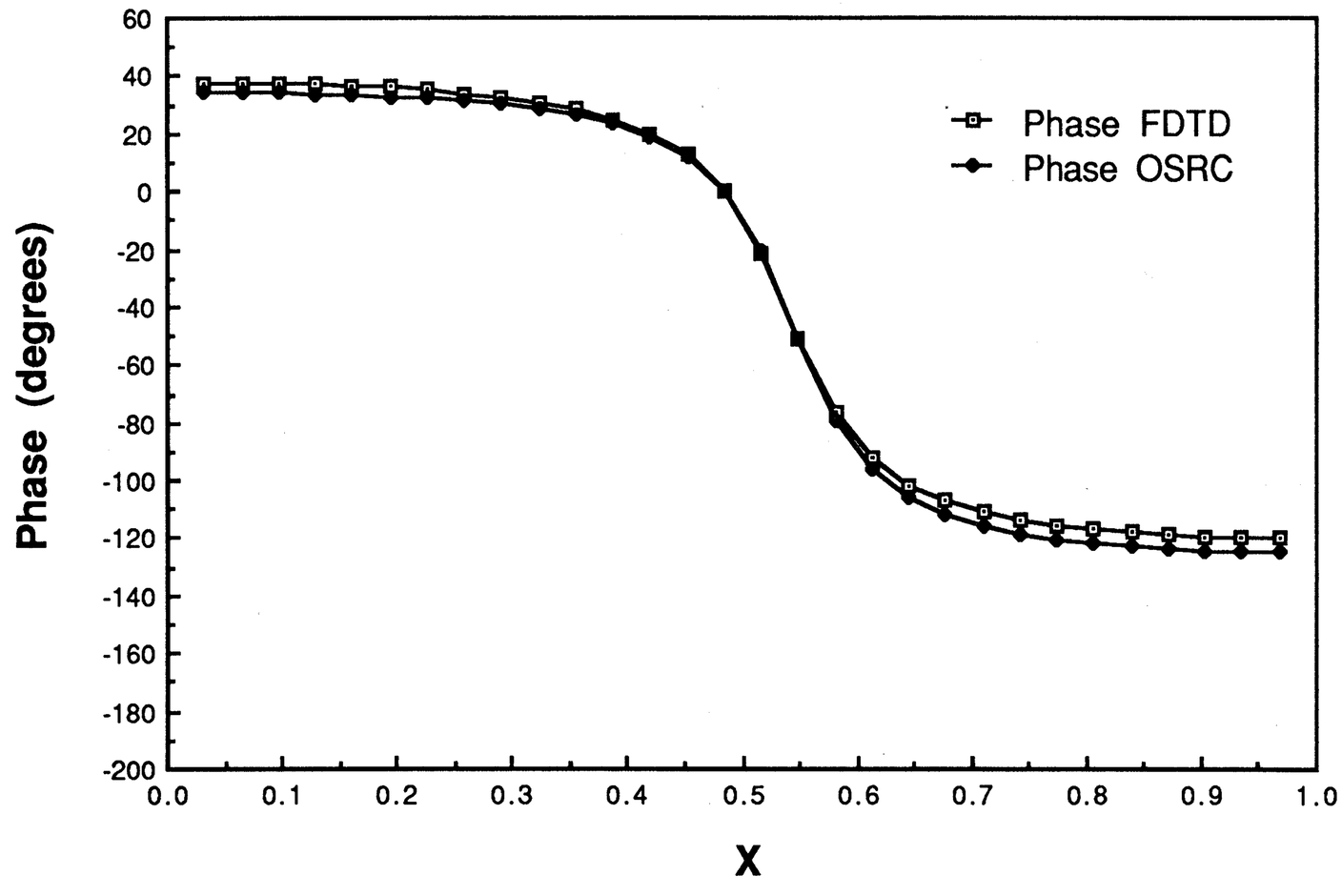

Fig. 11. Same as Fig. 9 except $\alpha = 30°$.

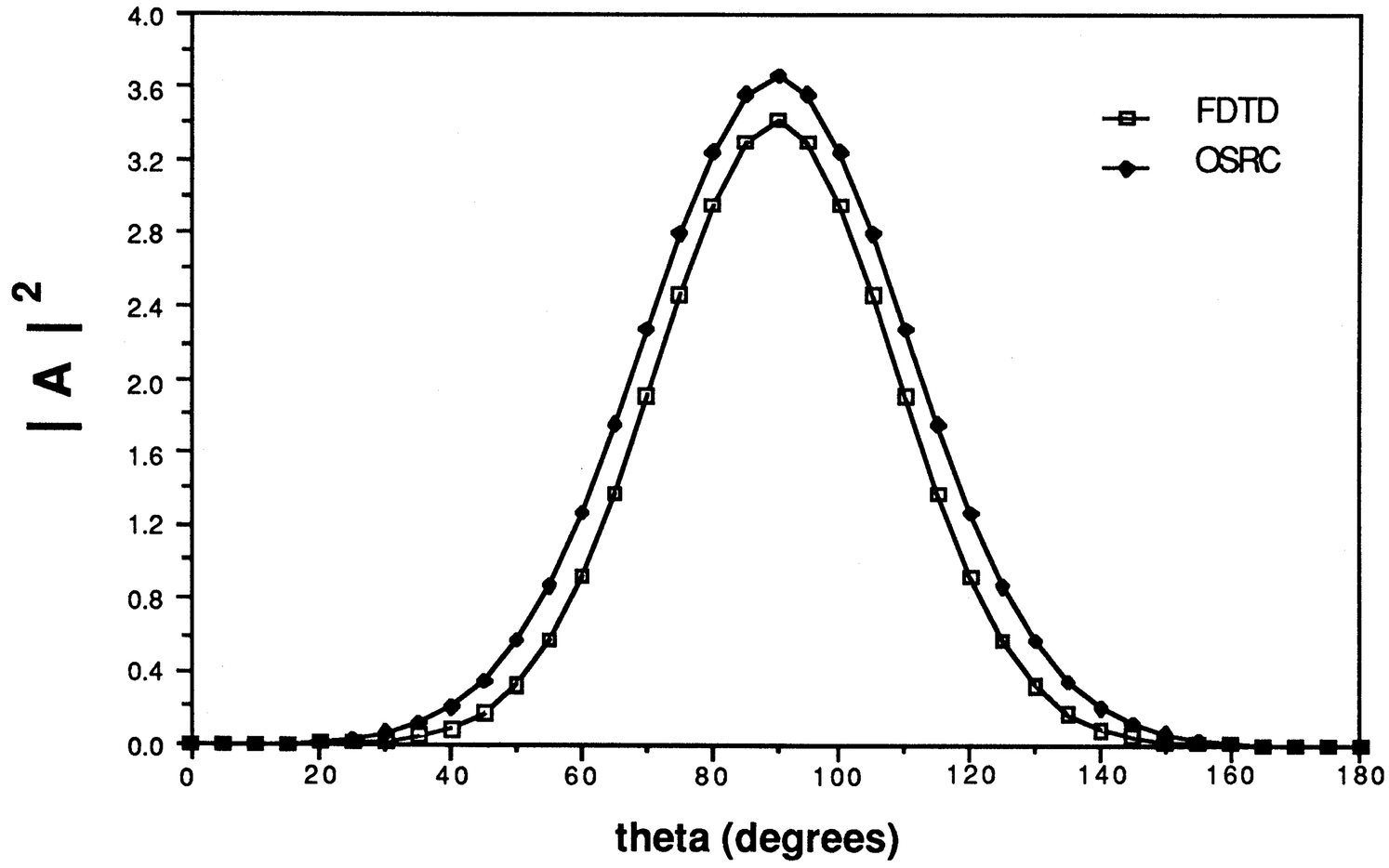

Fig. 12. Bistatic cross-section for the field scattered from the aperture of the cavity in the region $z<0$ for $\alpha=0°$. The angle θ is as shown in Fig. 1.

ture. The deviation between the $k^{c}_{n,m}$ and the real part of the complex eignefrequency, as predicted by the OSRC method, will be discussed in the next section.

5. Complex eigenfrequencies of the open cavity

The complex eigenfrequencies for the open cavity can be approximated using our OSRC

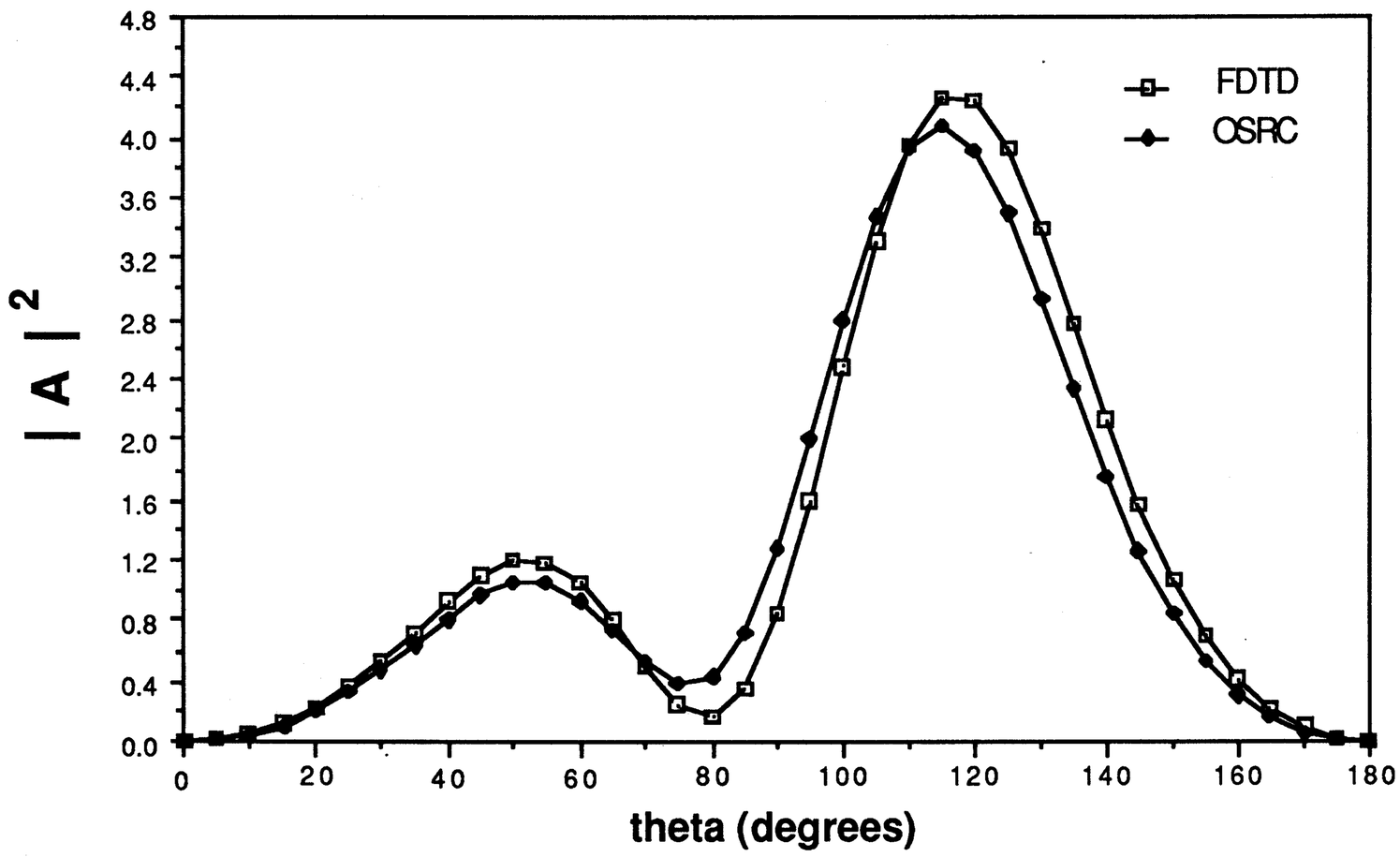

Fig. 13. Same as Fig. 12 except $\alpha=30°$.

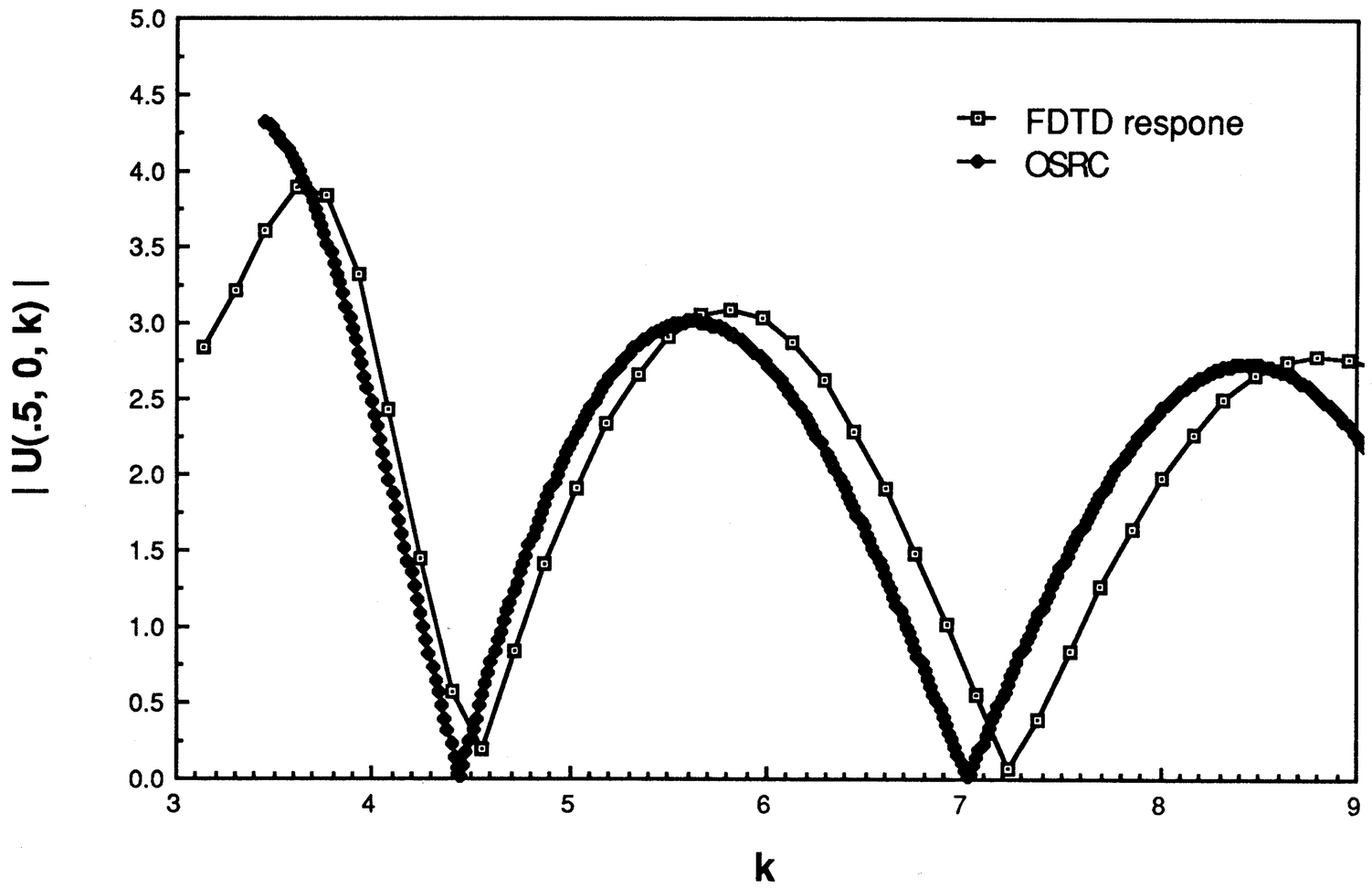

Fig. 14. Behavior of field magnitude as a function of wavenumber k at the mid-point of the cavity aperture ($\alpha = 0°$).

theory by setting the denominator of T_n equal to zero. Accordingly, setting $J_n = 0$ in (3.6b), solving for γ_n, and simplifying the resulting expression we obtain

$$\gamma_n = (k + k_n)^4/(n\pi)^4. \tag{5.1}$$

Inserting the change of variable

$$k = n\pi \cos\theta \tag{5.2}$$

into (2.6) and (5.1), we find that

$$\exp(\lambda \sin\theta) = \exp(4i\theta) \tag{5.3a}$$

where λ is defined by

$$\lambda = 2n\pi d. \tag{5.3b}$$

Equating the exponents in (5.3a), modulo 2π, and setting $\theta = x + iy$, we deduce that x and y satisfy the simultaneous equations

$$\cos x \sinh y = \frac{4x + 2m\pi}{\lambda}, \tag{5.4a}$$

$$\sin x \cosh y = -\frac{4y}{\lambda}. \tag{5.4b}$$

An approximate solution of the system (5.4) can be obtained when λ is large by observing that the right-hand sides of (5.4) are formally small. Accordingly, we replace $\sinh y$ by y, $\sin x$ by x, $\cos x$ by 1, and $\cosh y$ by 1, and obtain a linear system whose solution is

$$x = -\frac{8m\pi}{16 + \lambda^2}, \tag{5.5a}$$

$$y = \frac{2m\pi\lambda}{16 + \lambda^2}. \tag{5.5b}$$

Combining these results with the definition of θ and (5.2), and using the small argument approximation for the cosine, we deduce the approximation

$$k = n\pi\left\{1 - \frac{32\pi^2m^2}{(16+\lambda^2)^2} + \frac{2\pi^2m^2\lambda^2}{(16+\lambda^2)^2}\right\} + in\pi\left\{\frac{16m^2\pi^2\lambda}{(16+\lambda^2)^2}\right\} \tag{5.6}$$

We have also solved the nonlinear system (5.4) by employing a Newton–Raphson scheme using the approximation (5.5) as an initial guess. Once the solution was obtained, we set $\theta = x + iy$, inserted this complex number into (5.2), and separated the real and imaginary parts of k. The results of

Table 1

n	Complex eigenfrequencies for $m=-1$	
	Iterative solution of (5.4)	Approximate solution using (5.6)
1	3.773+i 0.9447	3.615+i 1.013
2	6.865+i 0.3758	6.865+i 0.4122
3	9.877+i 0.1923	9.883+i 0.2035
4	12.93+i 0.1148	12.93+i 0.1189

Table 2

n	Complex eigenfrequencies for $m=-2$	
	Iterative solution of (5.4)	Approximate solution using (5.6)
1	6.135+i 2.473	5.034+i 4.051
2	8.524+i 1.174	8.611+i 1.649
3	11.16+i 0.6620	11.26+i 0.8139
4	13.96+i 0.4161	14.02+i 0.4756

our effort are shown in Table 1 for $m=-1$, $n=1,2,3,4$, and in Table 2 for $m=-2$, $n=1,2,3,4$. Negative values for m were chosen to ensure that the imaginary part of k was positive. The first column in each table contains the roots generated by the iterative scheme while the second lists those obtained from (5.6). The two columns agree well for $m=-1$ but deviate, especially for $n=1$ and $m=-2$.

Finally, the deviation between the closed-cavity eigenfrequencies given by (4.1) and the real parts of k listed in Tables 1 and 2 differ by less than 2% for $n=2,3,4$ and by about 12% when $n=1$. The imaginary part of the eigenfrequencies, which measures the rate at which energy leaks out of the open cavity, decreases as m increases. This indicates that the higher modes are trapped longer in the resonator and agrees with a ray interpretation.

Acknowledgment

This work was sponsored in part by the National Science Foundation under Grant No. DMS-8700794.

References

[1] G.A. Kriegsmann, A. Taflove, and K.R. Umashankar, "A new formulation of electromagnetic wave scattering using an On-Surface Radiation Boundary Condition", *IEEE Trans. Antennas and Propagation AP-35*, 153-161 (1987).

[2] J.G. Blaschak, T.G. Moore, G.A. Kriegsmann, and A. Taflove, "Theory and application of radiation boundary operators", *IEEE Trans. Antennas and Propagation*, in press.

[3] G.A. Kriegsmann and T.G. Moore, "An application of the On-Surface Radiation Condition to the scattering of acoustic waves by a reactively loaded sphere", *Wave Motion 10*(3), 277-284 (1988).

[4] A.Q. Howard, "On the mathematical theory of electromagnetic radiation from flanged waveguides", *J. Math. Phys. 13*(4), 482-490 (1972).

[5] H.Y. Yee, L.B. Felsen, and J.B. Keller, "Ray theory of reflection from the open end of a waveguide", *SIAM J. Appl. Math. 16*(2), 268-300 (1968).

[6] L. Grun and S.W. Lee, "Transmission into staggered parallel-plate waveguides", *IEEE Trans. Antennas and Propagation AP-30*, 35-43 (1982).

[7] H. Shirai and L.B. Felsen, "Rays, modes, and beams for plane wave coupling into a wide parallel-plate waveguide", *Wave Motion 9*, 301-317 (1987).

[8] A. Taflove, "Application of the finite-difference time-domain method to sinusoidal steady-state electromagnetic penetration problems", *IEEE Trans. Electromag. Compat. EMC-22*, 191-202 (1980).

[9] A. Taflove, K.R. Umashankar, B. Beker, and F. Harfoush, "Detailed FD-TD analysis of electromagnetic field penetrating narrow slots and lapped joints in thick conducting screens", *IEEE Trans. Antennas Propag.*, in press.

[10] G.A. Kriegsmann and C.S. Morawetz, "Solving the Helmholtz equation for exterior problems with a variable index of refraction", *SIAM J. Sci. Stat. Comput. 1*, 371-385 (1980).

[11] A. Bayliss and E. Turkel, "Radiation boundary conditions for wave-like equations", *Comm. Pure Appl. Math. 23*, 707-725 (1980).

[12] B. Enquist and A. Majda, "Absorbing boundary conditions for the numerical simulation of waves", *Math. Comput. 31*, 629-651 (1977).